International Journal of
Geo-Information

MDPI

Article

Spatiotemporal Characteristics and Driving Force Analysis of Flash Floods in Fujian Province

Junnan Xiong [1,2], Quan Pang [1], Chunkun Fan [3], Weiming Cheng [2,4,5,*], Chongchong Ye [1], Yunliang Zhao [1], Yuanrong He [6] and Yifan Cao [1]

1. School of Civil Engineering and Architecture, Southwest Petroleum University, Chengdu 610500, China; Xiongjn@swpu.edu.cn (J.X.); 201822000590@stu.swpu.edu.cn (Q.P.); 201822000599@stu.swpu.edu.cn (C.Y.); z1377133206@gmail.com (Y.Z.); 201822000588@stu.swpu.edu.cn (Y.C.)
2. State Key Laboratory of Resources and Environmental Information System, Institute of Geographic Sciences and Natural Resources Research, CAS, Beijing 100101, China
3. Agriculture Research Institute, Tibet Academy of Agriculture and Animal Husbandry Sciences, Lhasa 850000, China; fanchunkun72@163.com
4. University of Chinese Academy of Sciences, Beijing 100049, China
5. Jiangsu Center for Collaborative Innovation in Geographical Information Resource Development and Application, Nanjing 210023, China
6. College of Computer and Information Engineering, Xiamen University of Technology, Xiamen 361024, China; 2012112001@xmut.edu.cn

* Correspondence: chengwm@lreis.ac.cn

Received: 31 December 2019; Accepted: 18 February 2020; Published: 23 February 2020

Abstract: Flash floods are one of the most destructive natural disasters. The comprehensive identification of the spatiotemporal characteristics and driving factors of a flash flood is the basis for the scientific understanding of the formation mechanism and the distribution characteristics of flash floods. In this study, we explored the spatiotemporal patterns of flash floods in Fujian Province from 1951 to 2015. Then, we analyzed the driving forces of flash floods in geomorphic regions with three different grades based on three methods, namely, geographical detector, principal component analysis, and multiple linear regression. Finally, the sensitivity of flash floods to the gross domestic product, village point density, annual maximum one-day precipitation (Rx1day), and annual total precipitation from days > 95th percentile (R95p) was analyzed. The analytical results indicated that (1) The counts of flash floods rose sharply from 1988, and the spatial distribution of flash floods mainly extended from the coastal low mountains, hills, and plain regions of Fujian (IIA2) to the low-middle mountains, hills, and valley regions in the Wuyi mountains (IIA4) from 1951 to 2015. (2) From IIA2 to IIA4, the impact of human activities on flash floods was gradually weakened, while the contribution of precipitation indicators gradually strengthened. (3) The sensitivity analysis results revealed that the hazard factors of flash floods in different periods and regions had significant differences in Fujian Province. Based on the above results, it is necessary to accurately forecast extreme precipitation and improve the economic development model of the IIA2 region.

Keywords: flash flood; spatiotemporal patterns; driving forces; geomorphic regionalization; sensitivity; Fujian Province

1. Introduction

A flash flood is a violent surface runoff of water caused by heavy precipitation in a small watershed with an area under 100 km^2. Flash floods are characterized by suddenness, severe damage, and strong destructiveness [1,2]. According to the statistics of the World Meteorological Organization, flash floods cause the highest casualties out of all flood-related disaster events, and flash floods rank among the top 10 in terms of property losses when taking into consideration all natural disasters in 75% of the countries affected [3]. In the United States, a total of 21,549 flash floods occurred from 2006 to 2010. These floods caused 224 injuries and 326 deaths [4]. The catastrophic flash flood in 1997 in Somalia caused 2311 deaths, accounting for approximately 18% of the total population affected [5]. In the Rubi River Basin in Spain, 441 deaths and losses of approximately 2650 million Euros were attributed to the flash floods that occurred in September 1962 [6]. China has a vast territory and a complex eco-geographic environment, and it is simultaneously affected by extreme weather, human social activities, and other factors [7,8]. Because of these conditions, China has undergone some of the most severe effects in the world due to flash floods [9]. Since the beginning of the 21st century, 80% of the total deaths from floods in China have been caused by flash floods [9]. In this context, the State Council approved the "National Flash Flood Disaster Prevention and Control Plan (NFFDPCP)" in October 2006 [10], and the "National Flash Flood Investigation and Evaluation Project (NFFIEP)" was launched in 2013 [11]. These programs provide a reliable data foundation for the monitoring and prediction of flash floods.

After reviewing previous studies, research on flash floods has focused on the following aspects: First, the risk assessment of flash floods, which includes hazard and vulnerability assessment [12,13]. These research studies were mainly conducted at the county and provincial scales [14–16]. Second, flash flood mechanisms, including the process of occurrence, development, and influence [6,17]. In particular, flash flood warning systems have been established based on these mechanism studies, which have been combined with the critical rainfall, critical water level, and other factors [18,19]. The scenario simulations of flash floods have been performed using the Mike Flood and Flood Area system by some researchers [20,21]. These studies have mainly been conducted on flash flood ditches or at a watershed scale [22,23]. Finally, some researchers have explored the spatiotemporal patterns and driving forces of flash floods [24,25]. The spatiotemporal pattern analyses were based on the historical spatiotemporal variation in a long time series. The conditions of the underlying surfaces, population activity distribution, and precipitation were selected for the driving force detection [25–27]. Moreover, a quantitative analysis was performed for the driving force of numerous factors that could contribute to understanding the formation of flash floods [28]. Generally, an inland province or a county was selected as the research object.

However, there are also some problems with the existing studies of the spatiotemporal patterns and driving factors for flash floods. First, some dynamic factors were reflected by static factors, and the aspect of the spatiotemporal variation of the dynamic factors was neglected. These dynamic factors include the population distribution, precipitation, vegetation cover, and land use. Therefore, the corresponding results were not sufficiently accurate and objective. Second, a few studies have revealed the effect of human activities on flash floods, but research on the responses of flash floods to the gradual intensifying of human activity and precipitation is still rare. Finally, previous studies have detected the interaction between two driving factors [28,29], but the results did not sufficiently reflect the contribution rate of each driving factor. Therefore, research from the perspective of the interaction of multiple factors with flash floods is highly recommended. In particular, Fujian Province, at the forefront of China's reform and opening-up, has a high population density and developed economy [30], but it is greatly affected by extreme precipitation events, such as tropical cyclones [31]. Additionally, the characteristics of flash floods in Fujian Province are still unknown. Furthermore, the distributions of the precipitation and human activities are constrained by the topographic forms in Fujian Province [32]. Overall, it is urgent to know about the spatial distribution difference from coastal to inland.

Thus, in this study, a long-time series of flash flood events was used to analyze the spatiotemporal variation in Fujian Province from 1951 to 2015 using a Mann-Kendall test and the standard deviation ellipse method (SDE). Then, a geographical detector model, principal component analysis (PCA), and multiple linear regression (MLR) were adopted to quantitatively evaluate the single factor explanatory power and contribution rate of the interaction of multiple driving factors (include multi-periods dynamic factors) with the spatial patterns of flash floods based on a three-grade geomorphic regionalization (GR). Lastly, a geographically and temporally weighted regression (GTWR) model was adopted to explore the sensitivities of flash flood to population (POP) density, gross domestic product (GDP) density, village point density (VPD), and rainstorms (PII). The main objective was to provide primary references for the prevention of flash floods.

2. Materials and Methods

2.1. Study Area

Fujian Province (115°40′–120°30′ E, 23°30′–28°20′ N) is situated on the southeastern coast of China (Figure 1), on the edge of the Asian continent, facing east to the Taiwan Strait. As the forefront of China's reform and opening-up, Fujian Province is characterized by a developed economy and high population density. The population and the GDP density were 39.11 million and 3.58 trillion RMB at the end of 2017, respectively [33]. Moreover, Fujian Province has complex terrain, and the western and central mountain ranges are parallel to the coastal hills, which constitute the topographic skeleton of Fujian Province [34]. It has a dense water system with numerous rivers, and the river network density is 0.1 km/km^2. The soil structure is loose in the north-central region, with strong weathering and low sloping hills in the southeast [35]. In terms of climatic conditions, Fujian Province is located on the western coast of the Pacific Ocean with a subtropical ocean monsoon climate, and the area is greatly impacted by tropical cyclones. In this region, the light is sufficient and precipitation is abundant, with an annual average temperature range of 17 °C–21 °C and an annual precipitation range of 1400–2000 mm [36]. According to previous research, approximately 95% of the land area and 84% of the population are threatened by flash floods [37]. Thus, it is one of the areas that is the most vulnerable to the frequently occurring flood floods in China.

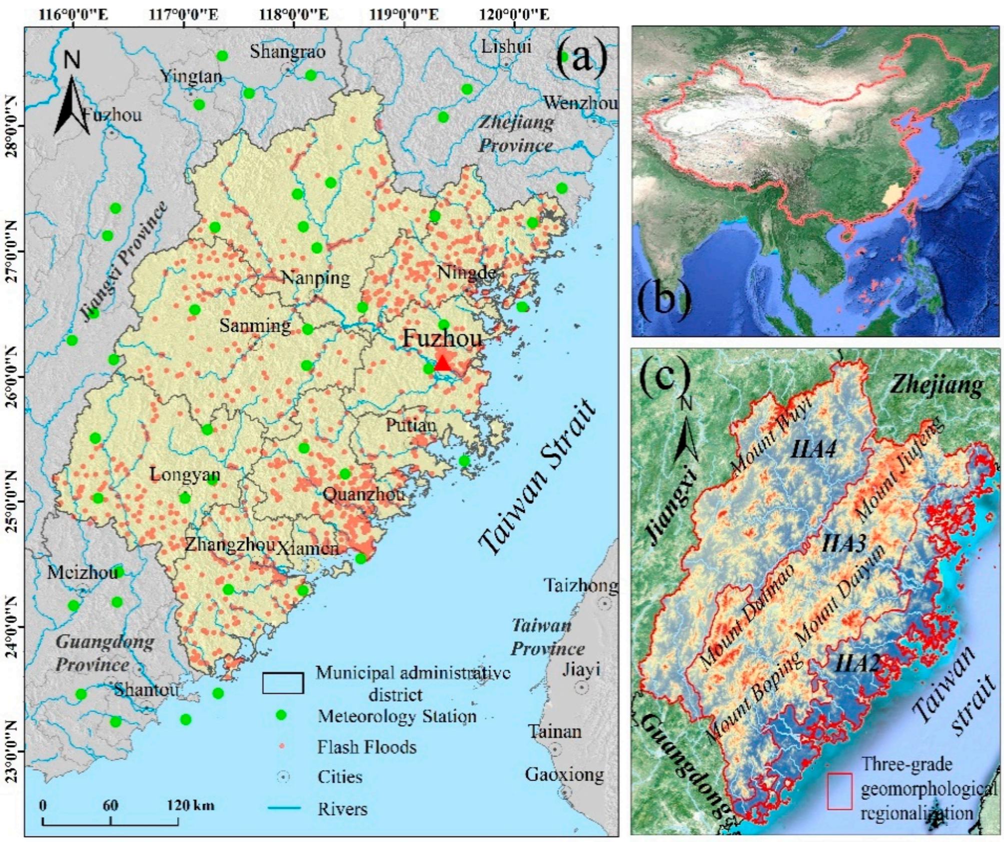

Figure 1. The study area: (**a**) The spatial distribution of the flash floods in Fujian Province; (**b**) The geographical position of Fujian in China; (**c**) Three-grade geomorphic regionalization in Fujian Province.

2.2. Data

In this study, the flash flood data were obtained from the NFFIEP dataset. This dataset includes 30 provinces in China, with a total land area of 7.55 million km^2 and a population of nearly 900 million. Moreover, the attribute data (e.g., position, and time) of the flash floods were collected in the form of points [2]. In this study, the data were collected based on three aspects: human activity indicator, precipitation indicator, and surface environmental indicator. The datasets are listed in Table 1.

The human activity factors included the population density (POP; unit: person/km^2), GDP density (GDP; unit: yuan/km^2), road density (RD; unit: km/km^2), and village point density (VPD; unit: village/km^2). These indicators reflected the intensity of human activity in Fujian Province.

The precipitation indicators were calculated from daily observations of precipitation. The daily precipitation data for 50 meteorological stations from 1951 to 2015 in Fujian Province and its surroundings were obtained from the National Meteorological Information of China (CMA) [38], and the data were used to analyze the spatiotemporal variation of precipitation in Fujian Province. In addition, according to the daily precipitation, four precipitation indicators were extracted: annual maximum one-day precipitation (Rx1day; mm), annual total precipitation from days > 95th percentile (R95p; mm), annual total precipitation from days > 99th percentile (R99p; mm), annual count when the precipitation was ≥ 50 mm (P50; days). These factors were recommended by the Expert Team on Climate Change Detection and Indices (ETCCDI) [39]. These precipitation indicators were used to reflect the impact of precipitation intensity on flash floods in Fujian.

The surface environment indicator included the vegetation fractional cover (VFC; unitless), elevation (ELE; unit: m), land use (LU; unitless), soil texture (ST; unitless), and formation lithology (FL; unitless). Among them, the ELE was extracted from the digital elevation model (DEM) that was obtained from the Geospatial Data Cloud site, Computer Network Information Center, Chinese Academy of Sciences (GDC) [40]. The VFC, LU, ST, and FL were collected from the Data Center for Resources and Environmental Sciences, Chinese Academy of Sciences (RESDC) [41].

Furthermore, the three-grade geomorphic regionalization (GR) was derived from the State Key Laboratory of Resources and Environmental Information System, Institute of Geographic Sciences and Natural Resources Research. The three-grade GR in Fujian Province was divided into the coastal low mountains, hills and plain regions of Fujian (IIA2); low-middle mountains, hills and valley regions in central Fujian (IIA3); and the low-middle mountains, hills and valley regions in Wuyi mountains (IIA4).

Table 1. List of data used.

Parameters	Scale or Resolution	Time	Date Sources
Flash floods	1:50,000	1951–2015	NFFIEP
Small watershed	1:50,000	2014	NFFIEP
Population density	1 km × 1 km	1990, 1995, 2000, 2005, 2010, 2015	RESDC
GDP density	1 km × 1 km	1990, 1995, 2000, 2005, 2010, 2015	RESDC
Village point	1:50,000	2014	NFFIEP
Road density	1:50,000	2014	NFFIEP
Daily precipitation	—	1951–2015	CMA
Vegetation fractional cover	1 km × 1 km	1995, 2000, 2005, 2010, 2015	RESDC
DEM	3 0m × 30 m	2009	GDC
Land use	1 km × 1 km	1995, 2010	RESDC
Soil type	1 km × 1 km	2010	RESDC
Formation lithology	1:500,000	2013	RESDC

2.3. Methodology

2.3.1. Spatiotemporal Analysis

(1) Mann-Kendall (M-K) test

For temporal pattern analysis, the M-K statistical test has been recognized and used in many studies [42], and it is widely used in time-series trend analysis for hydrology, meteorology, and natural disaster studies [43]. In this study, the M-K test was used to analyze the temporal variation of flash floods from 1951 to 2015 and to determine the mutation point, which is the time when the variation trend of flash floods changes. Among them, UF follows the normal distribution, which is a statistical sequence calculated according to time series, and UB is a statistical sequence calculated according to inverse time series. If the value of the UF is greater than 0, it indicates that the sequence is in an upward trend. If it is less than 0, it means a downward trend. When the value exceeds the critical line ($P = 0.05$), it indicates that the rising or falling trend is significant. If the UF and UB curves intersect, the value of the intersection point is the mutation point. Detailed information regarding the M-K test has been described in previous studies [44].

(2) Standard deviation ellipse method (SDE)

The SDE method was proposed by Lefever in 1926 [45]. It is an effective method for analyzing the spatial variation of point factors [46]. It is a simple model that is embedded in ArcGIS 10.5 software (ESRI, Inc., Redlands, CA, USA), with parameters that include the center point, azimuth, and area. The center point is used to reflect the center position of the geographic features and their evolution. The azimuth reflects the main trend direction of the geographical features in the spatial distribution. The area represents the concentration or divergence of the geographical features in the spatial distribution. In this study, the SDE method was used to reveal the directional trend and hence the degree of spatial dispersion of flash floods from the 1950s to the 2010s in Fujian Province.

2.3.2. Driving Factor Analysis

In this study, 13 driving factors were selected from the categories of human activity, precipitation, and the surface environment. Moreover, their explanatory power for the flash floods in Fujian Province was analyzed. A driving force analysis was performed for the period from 1981 to 2015, and the 35 years of the study period were divided into two periods: 1981 to 2000 (D1) and 2001 to 2015 (D2). In particular, the variations in the soil, vegetation, climate, hydrology, and human activities were constrained by the geomorphologies at different scales [47,48]. In this study, we analyzed the relationship between flash floods and the driving factors in the three-grade GR, which was proposed in previous research [49]. We generated 3000 random points in Fujian Province. The values for the kernel density and the driving factors for flash floods in the three GRs were extracted by these random points. Subsequently, the extracted data were divided into 10 levels using the "Natural Breaks" method in ArcGIS (except type variables: land use, soil texture). Furthermore, the average value of each driving factor was adopted to calculate the driving force of each driving factor on the flash flood.

(1) Land use (LU):

The runoff conditions varied greatly for different land uses, and a runoff coefficient was adopted to differentiate the types of land use. According to previous studies [50,51] and standards implemented according to the "Code for Design of Building Water Supply and Drainage of China (GB 50015-2003)" and the "Code for Design of Outdoor Wastewater Engineering of China (GB 50014-2006)" [51], ten types of land use were selected and given different runoff coefficients, as listed in Table 2:

Table 2. Land use types and corresponding coefficients.

Land Use Types	**Forest**	**Shrub**	**Herbaceous**	**Sparse Vegetation**	**Cropland**
Runoff Coefficients	0.15	0.18	0.2	0.45	0.6
Land Use Types	**Mangrove**	**Wetland**	**Bare area**	**Urban**	**Water**
Runoff Coefficients	0.4	0.5	0.7	0.9	1

(2) Soil Texture (ST)

Texture is an important property of soil that represents the relative proportions of the different particle sizes of the particles in the soil and is determined by the generation of surface runoff and the process of flooding [15,52]. In this study, based on previous studies, and as described by the Harmonized World Soil Database [51], different soil textures were given corresponding codes. In particular, the larger code values indicated stronger infiltration capabilities, as shown in Table 3.

Table 3. Soil textures and codes for the infiltration capacities.

Soil Texture Types	**Silty-Clay-Loam**	**Heavy-Clay-Loam**	**Clay-Loam**	**Silt-Loam**	**Sandy-Clay**
Codes	1	2	3	4	5
Soil Texture Types	**Loamy-clay**	**Loam**	**Sandy-clay-loam**	**Sandy/loamy sand**	**Water**
Codes	6	7	8	9	10

(3) Calculation of the precipitation indicator

Flash floods are often caused by short convective events, such as sub-daily precipitation and sub-daily extreme precipitation events. However, sub-daily precipitation data were not available for this study area. Therefore, daily precipitation data were used to calculate the four precipitation indicators (R95p, R99p, Rx1day, and P50) using the specially designed software RClimDEX (1.0) [53]. In particular, according to the definition of the "WMO Guidelines on the Calculation of Climate Normals (2017 edition)", the precipitation standard normal (averages of the precipitation data computed for the following consecutive periods of 30 years: 1 January 1981–31 December 2010, 1 January 1991–31 December 2020, and so forth) was used to analyze the temporal variation of precipitation in Fujian Province, and these four precipitation indicators were calculated as period averages (averages of climatological data computed for any period of at least ten years starting on 1 January of a year ending with the digit 1). Then, the four precipitation factors for 50 meteorological stations were interpolated based on the kriging interpolation method in ArcGIS 10.5 software, with a resolution of 1 km × 1 km. Specifically, 45 meteorological stations were used as interpolation samples. The rest of the stations were test samples, and the root mean square error (RMSE) was used as the accuracy assessment.

(4) Geographical detector

A geographical detector is a typical method used to detect spatial stratified heterogeneity and to reveal the correlation between two variables [54]. The basic idea of a geographical detector is that if the spatial pattern of an independent variable (e.g., precipitation) is similar to that of a dependent variable (e.g., flash flood density), this variable contributes to a certain amount of risk [55]. In this study, a geographical detector was adopted to explore the explanatory power of driving factors for flash floods in Fujian Province, and the Q value was used to measure the explanatory power of the various driving factors of flash floods. The formula is as follows:

$$Q = 1 - \frac{\sum_{h=1}^{n} N_h \sigma_h^2}{N\sigma^2}, \tag{1}$$

where n is the number of units in the study region, σ^2 denotes the variance of the driving factor, and N signifies the size of the study area. $Q \in (0, 1)$, $Q = 1$ indicates that the spatial patterns of flash floods were completely determined by the driving factors, while $Q = 0$ indicates that there was no association between the flash flood and the influential factors [56].

(5) Interaction of multiple factors for the flash floods

The occurrence of flash floods is the result of the interaction of two or more factors. Therefore, we adopted a combination of principal component analysis (PCA) and multiple linear regression (MLR) to explore the contribution rate of multiple factors to flash floods. PCA is a traditional multivariate technique. Its goal is to reduce the dimensionality of multiple variables and the difficulty of data analysis; detailed information about PCA has been described in previous studies [57]. The number of principal components was determined by the total variance, which was greater than 85%. Furthermore, two R packages ("psych" and "FactoMineR") were adopted to calculate the contribution rate of the principal components to flash floods. MLR is a typical statistical tool that can be performed to measure the correlations between two or more variables and to make predictions by using the relationship [58]. In this study, the results of the PCA were used as the input variables of MLR, and they were used to calculate the contribution rate of a single principal component or multiple principal components.

2.3.3. Sensitivity Analysis

The sensitivity of flash floods refers to the intensity of each flash flood event affected by driving factors. In this study, the geographically and temporally weighted regression model (GTWR) was adopted to calculate the sensitivity of a flash flood. This model was improved by Huang et al. based on the GWR [59,60]. The GTWR model is presented as follows:

$$y_i = \beta_0(\mu_i, v_i, t_i) + \sum\nolimits_k \beta_k(\mu_i, v_i, t_i) X_{ik} + \varepsilon_i, \tag{2}$$

where (u_i, v_i, t_i) are the spatiotemporal coordinates of the ith flash flood point; β_0 (u_i, v_i, t_i) is the regression constant of the ith flash flood point, which is the constant term of the GTWR; X_{ik} is the value of the independent variable X_i at the ith flash flood point, which is the value of each quantitative standard in the index system of the GTWR; ε_i denotes the residual of the GTWR; and β_k (u_i, v_i, t_i) is the kth regression parameter of the ith flash flood point, which is the weight of (u_i, v_i, t_i). The estimates of β_k (u_i, v_i, t_i) are as follows:

$$\hat{\beta}(\mu_i, v_i, t_i) = \left(X^T W(\mu_i, v_i, t_i) X\right)^{-1} X^T W(\mu_i, v_i, t_i) y, \tag{3}$$

where W (u_i, v_i, t_i) is the spatiotemporal weight matrix, the diagonal elements of which are indicated as the geographical weighting of the ith observation, and the off-diagonal elements are indicated as zero [61,62]. The parameters R^2 adjusted and coefficients of the GTWR represent the degree of data fitting and the level of sensitivity, respectively. The sensitivity was divided into four levels, as listed in Table 4:

Table 4. Coefficients (Coe) corresponding to the sensitivity levels.

Coefficients	Sensitivity Level	Description
Coe ≤ 0	Insensitive	This indicates that the changes in the flash floods and driving factors did not have any synchronized characteristics.
0 < Coe ≤ 0.04	Low Sensitivity	This indicates that the flash floods had low sensitivity to the variation of the driving factors.
0.04 < Coe ≤ 0.05	Moderate Sensitivity	This indicates that flash floods had moderate sensitivity to the variation of the driving factors.
Coe ≥ 0.05	High Sensitivity	This indicates that flash floods had high sensitivity to the variation of the driving factors.

3. Results

3.1. Spatiotemporal Pattern of Flash Floods

3.1.1. Temporal Change

To investigate the variation of flash floods in the time series from 1951 to 2015, an analysis was performed on the three time-scales: monthly, yearly, and interdecadal. As shown in Figure 2a, the results indicated that the temporal variation of the flash floods in Fujian Province was slightly reduced (slope = −0.289) from 1951 to 1980 but then rapidly increased (slope = 2.287) from 1981 to 2015. Furthermore, for the periods 1951–1952, 1957–1970, and 1983–2015 (Figure 2b), all the UF values were positive (the average values were 0.5, 0.9, and 3.081, respectively). This signified that during these periods, the frequency of flash floods was on the rise, and for the remaining periods, there was a decrease. Specifically, the mutation point (the intersection point of UF and UB) occurred in 1988 (Figure 2b), and it showed that flash floods steadily increased after 1988. In addition, the values of the UF were greater than the upper limit ($P = 0.05$) in 1995, which signified that the counts of the flash floods sharply increased after 1995. In the seven periods from the 1950s to 2010s (Figure 2d), the number of flash floods of the 1990s, 2000s, and 2010s accounted for 75.3% of the total, with a significant increasing trend of flash floods ($R^2 = 0.72$). An obvious seasonal variation occurred (Figure 2d–f), and there were significant differences in the time and quantity of the occurrence of flash floods in different GRs. In the IIA2 region, flash floods mainly occurred from May to September. For the IIA3 region, the flash floods were mainly concentrated in June and August. Regarding the IIA4 region, the largest number of flash floods occurred in June.

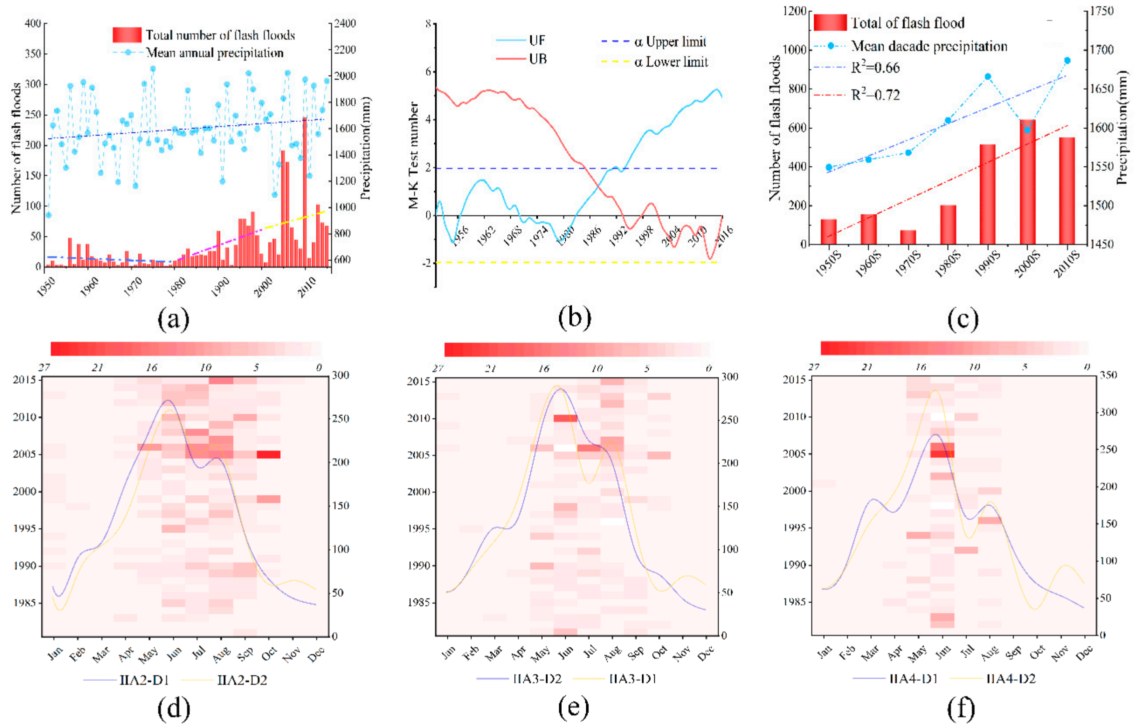

Figure 2. (**a**) The annual number of flash floods and the mean annual precipitation in Fujian Province from 1951 to 2015 and (**b**) flash flood mutation analysis using the Mann-Kendall test. (**c**) The interannual number of flash floods and the mean interannual precipitation in Fujian Province. (**d**–**f**) are the monthly number of flash floods in IIA2, IIA3, and IIA4, respectively. The curves represent the mean monthly precipitation of two periods under different geomorphological regionalization.

3.1.2. Spatial Change

The SDE was performed to measure the spatial pattern of flash floods from the 1950s to the 2010s. As illustrated in Figure 3, from the 1950s to the 2010s, the azimuth of the SDE ranged from 21.767° to 41.157°, and the SDE area ranged from 24,602.69 km^2 to 65,099.24 km^2. In addition, from the point of gravity shift, the gravity center of the flash floods was mainly located in the Putian, Quanzhou, Fuzhou, and Sanming regions, with a shift of the gravity center from central and eastern areas to the northwestern area of Fujian. In general, the number of flash flood events increased obviously after the 1980s, and the spatial distribution of flash floods mainly extended from IIA2 to IIA3 and to IIA4 from the 1950s to the 2010s.

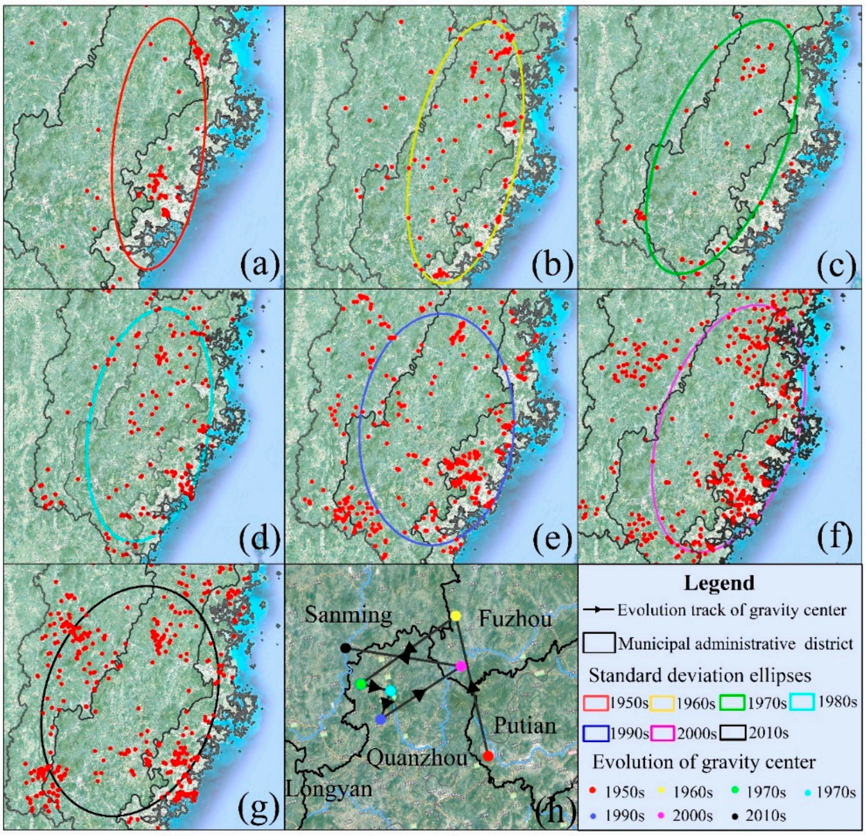

Figure 3. Distribution and gravity center evolution of flash floods during seven periods from the 1950s to the 2010s in Fujian Province. (**a**–**g**) are the spatial distributions of Fujian's flash floods represented in the seven periods from the 1950s to the 2010s. (**h**) is the evolution track of the gravity center.

3.2. *Driving Factors of Flash Floods in Fujian Province*

3.2.1. Distribution of the Major Driving Factors

(1) Precipitation Factors

The temporal variation of the precipitation from 1951 to 2015 exhibited an overall increasing trend (Figure 2a). For the seven periods from the 1950s to the 2010s (Figure 2c), there was an obvious increasing trend of precipitation (R^2 = 0.66). Precipitation standard normals were 1563.156 mm per year, 1580.379 mm per year, 1617.906 mm per year, 1629.948 mm per year, and 1642.282 mm per year in periods 1951–1980, 1961–1990, 1971–2000, 1981–2010, and 1986–2015, respectively. These analyses further proved that the precipitation was on the rise. Furthermore, the months and the precipitation peaks of the heavy precipitation had significant differences for the different GRs in the IIA2, IIA3, and IIA4 regions, and the precipitation was mainly concentrated in April to September, May to August, and May to June, respectively. As exhibited in Figure 4, in the D1 and D2 periods, the average RMSE values were 3.39 and 3.32, respectively, and the interpolation result could accurately represent the spatial distribution of the precipitation. For the spatial distribution, Figure 4a,b,e,f indicates the increase in the intensity and the larger range of influence of R95p and R99p from D1 to D2. Figure 4c,d reflects the fact that the Rx1day shifted from the southeast to northeast from D1 to D2. Figure 4c,d illustrates the annual count when the precipitation ≥ 50 mm decreased from D1 to D2.

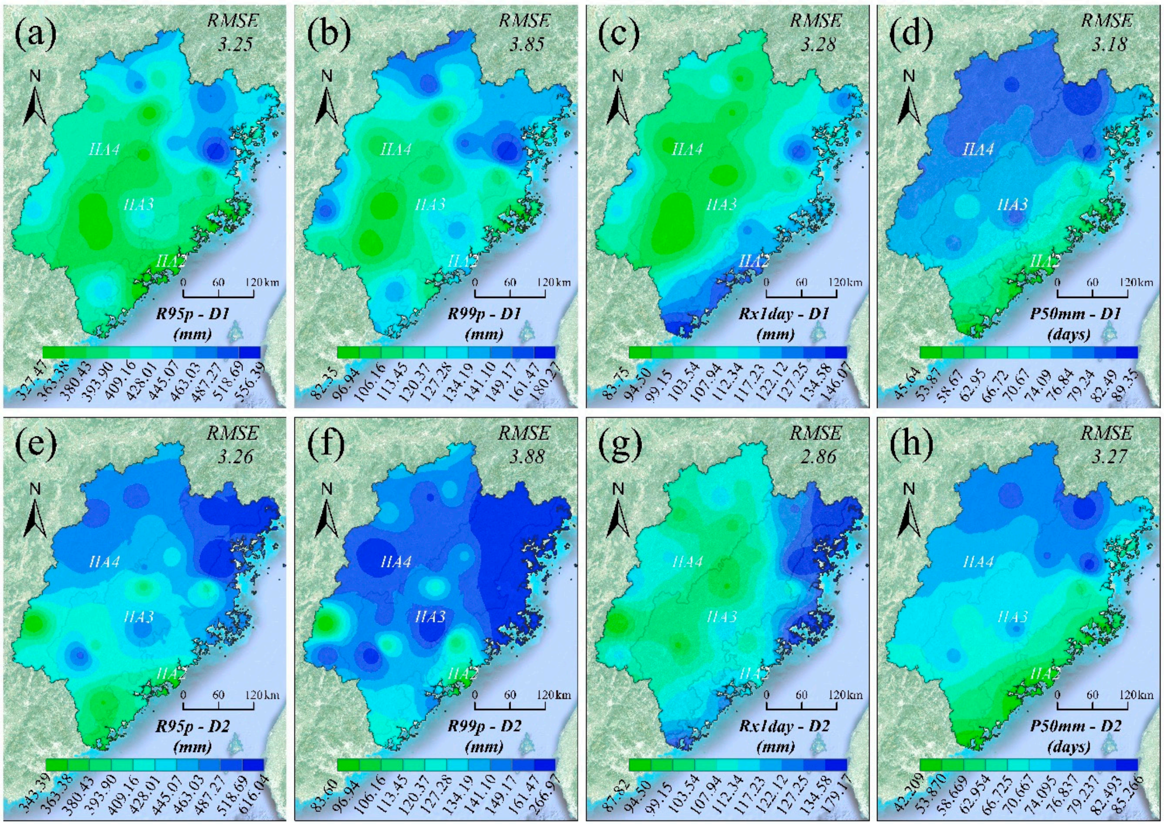

Figure 4. Spatial distribution of the four precipitation indicators in Fujian Province during D1 (1981 to 2000) and D2 (2001 to 2015): (**a**) R95p in D1, (**b**) R99p in D1, (**c**) Rx1day in D1, (**d**) P50 in D1, (**e**) R95p in D2, (**f**) R99p in D2, (**g**) Rx1day in D2, and (**h**) P50 in D2.

(2) Human Activity Factors

In this study, we adopted the VPD, RD, GDP, and POP density to reflect the spatial distribution and intensity of human activity. As displayed in Figure 5, the most concentrated regions of human activity were mainly distributed in coastal regions, and these regions were mainly located in IIA2, with dense villages, road networks, population, and a developed economy. In particular, the GDP increased rapidly (Figure 5b,e), with a significant change in the spatial distribution of Longyan, and there was obvious growth in Fujian, Quanzhou, Putian, and Xiamen. In addition, the spatial distribution of the POP was almost identical in the D1 and D 2 periods, except for the Longyan areas. However, the difference in the POP density was obvious, in Fujian (Figure 5c,f), Quanzhou, Sanming, Longyan, Putian, and Xiamen, with a significant increase from D1 to D2.

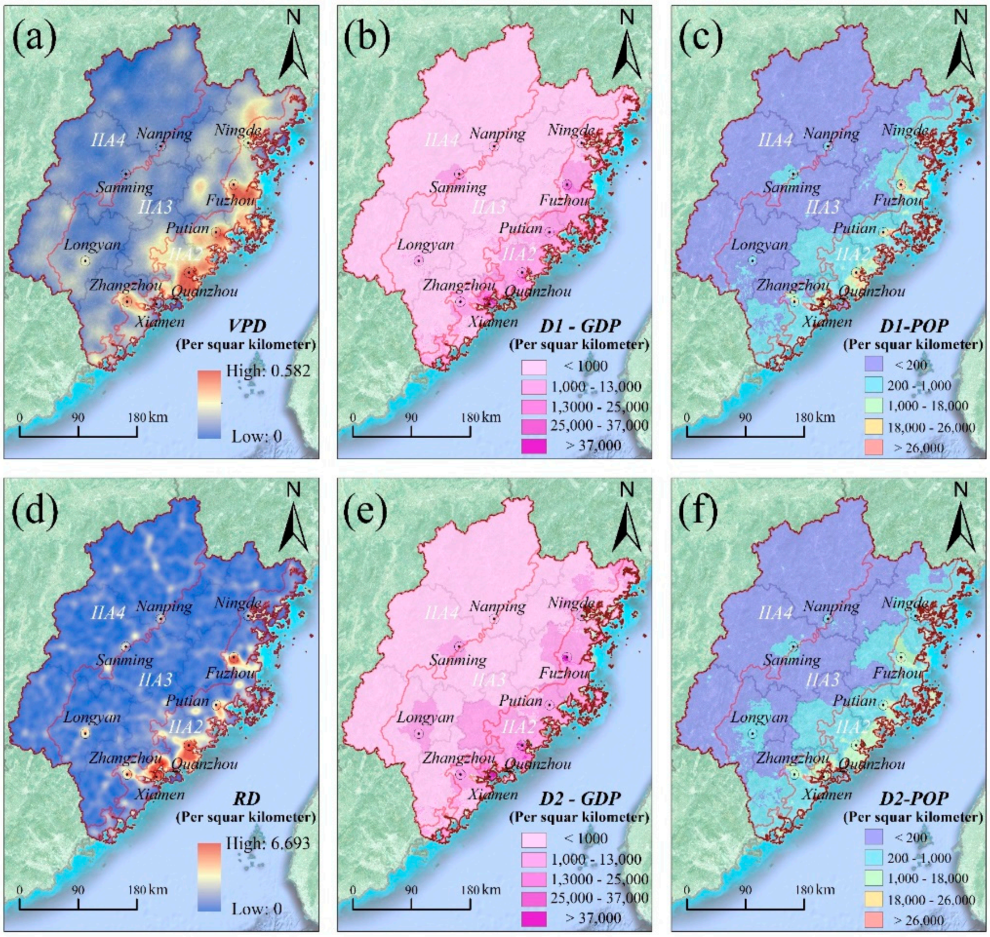

Figure 5. (**a**) VPD and (**d**) RD display the spatial distribution of the VPD and RD, respectively; (**b**,**c**) present the spatial distributions of GDP and POP in D1, respectively; (**e**,**f**) exhibit the spatial distributions of GDP and POP in the D2 period, respectively.

3.2.2. Driving Factor Detection

In this study, the explanatory power of the various driving factors with respect to the spatial patterns of the flash floods from 1981 to 2015 is listed in Table 5. Furthermore, results of the interaction of various driving factors for flash floods for different GRs from D1 to D2 by PCA and MLR are illustrated in Figure 6.

For the IIA2 region: In the D1 period, the highest Q value was that of R99p (Q = 0.483, P < 0.01), followed by R95p (Q = 0.342, P < 0.01), VPD (Q = 0.318, P < 0.01), and POP (Q = 0.293, P < 0.01). According to Figure 6a,d, the interaction of *Dim 1* and *Dim 2* contributed the highest R^2 value (R^2 = 0.332), which was attributed to the driving factors of the VPD (18.44%), GDP (16.27%), P50 (15.62%), POP (14.10%), R95p (11.28%), and RD (10.85%). In the D2 period, the VPD (Q = 0.424, P < 0.01), R99p (Q = 0.396, P < 0.01), Rx1day (Q = 0.392, P < 0.01), and GDP (Q = 0.246, P < 0.01) were the main driving factors. As presented in Figure 6b,e, the highest R^2 value (R^2 = 0.429) was a consequence of the interaction of *Dim 1* and *Dim 3*, and the main contributing driving factors were VPD (14.01%), GDP (13.86%), POP (13.26%), R99p (13.11%), R95p (11.77%), RD (11.48%), and Rx1day (11.18%).

The IIA3 region: In the D1 period, the highest Q values were those of the P50 (Q = 0.208, P < 0.01), R95p (Q = 0.197, P < 0.01), R99p (Q = 0.181, P < 0.01), and Rx1day (Q = 0.152, P < 0.01). As illustrated in Figure 6c,f, the interaction of *Dim 1*, *Dim 2*, *Dim 3*, and *Dim 4* contributed the highest R^2 value (R^2 = 0.126), which accounted for the driving factors of the VPD (18.24%), POP (17.06%), R99p (14.44%), R95p (14.44%), GDP (12.86%), and Rx1day (12.47%). In the D2 period, the highest Q values of the driving factors exhibited the following rankings: Rx1day (Q = 0.344, P < 0.01), VPD (Q = 0.337,

$P < 0.01$), R99p ($Q = 0.304$, $P < 0.01$), R95p ($Q = 0.304$, $P < 0.01$), P50 ($Q = 0.261$, $P < 0.01$), and POP ($Q = 0.211$, $P < 0.01$). As displayed in Figure 6g,j, the highest R^2 value ($R^2 = 0.427$) was due to the interaction of *Dim 1*, *Dim 2*, *Dim 3*, and *Dim 4*, and the main contributing driving factors were the VPD (20.08%), Rx1day (19.82%), POP (16.25%), R99p (12.95%), R95p (11.49%), and GDP (10.04%).

The IIA4 region: In the D1 period, the highest Q values were those for the GDP ($Q = 0.208$, $P < 0.01$), Rx1day ($Q = 0.238$, $P < 0.01$), R95p ($Q = 0.232$, $P < 0.01$), R99p ($Q = 0.190$, $P < 0.01$), and P50 ($Q = 0.179$, $P < 0.01$). As illustrated in Figure 6h,k, the interaction of *Dim 1*, *Dim 2*, and *Dim 3* contributed the highest R^2 value ($R^2 = 0.175$), which was attributed to the driving factors of R99p (30.52%), Rx1day (27.27%), R95p (26.30%), POP (14.94%), and P50 (11.69%). In the D2 period, P50 ($Q = 0.285$, $P < 0.01$), Rx1day ($Q = 0.281$, $P < 0.01$), GDP ($Q = 0.162$, $P < 0.01$), VPD ($Q = 0.138$, $P < 0.01$), and POP ($Q = 0.118$, $P < 0.01$) were the main driving factors. As displayed in Figure 6i,l, the highest R^2 value ($R^2 = 0.033$) was a consequence of the interaction of *Dim 1*, *Dim 2*, and *Dim 3*, and the main contributing driving factors were R95p (46.22%), P50 (44.96%), R99p (43.28%), Rx1day (38.66%), and RD (16.81%).

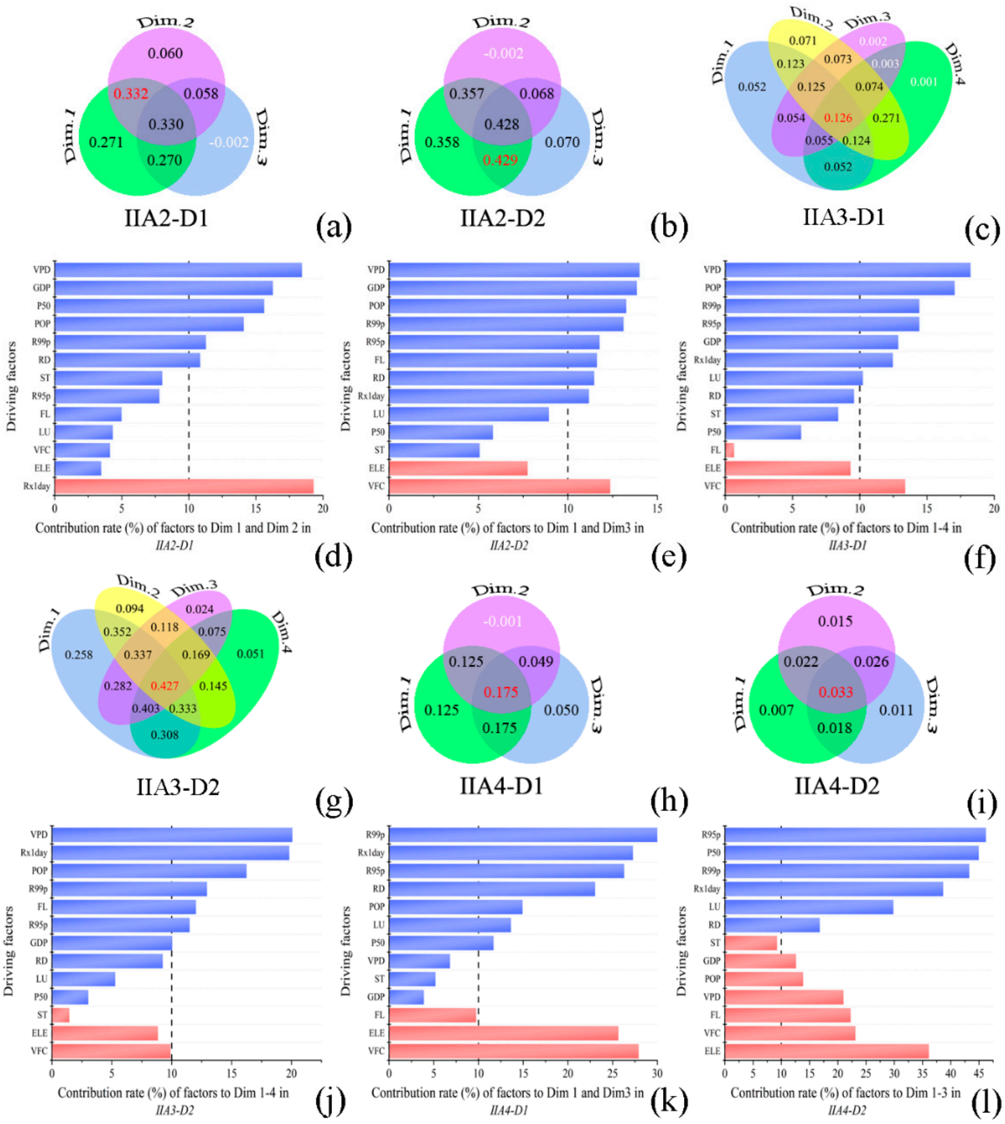

Figure 6. Interaction detection analysis based on principal component analysis and multiple linear regression in different geomorphological regions from D1 to D2. (**a**,**c**,**h**) are R^2 values of the multiple linear regression (MLR) of the principal components for flash floods in the IIA2, IIA3, and IIA4 regions

in the D1 period. (**d**,**f**,**k**) are the contribution rates of the driving factors to the principal components in the IIA2, IIA3, and IIA4 regions in the D1 period. (**b**,**g**,**i**) are R^2 values of the MLR of the principal components of the flash floods in the IIA2, IIA3, and IIA4 regions in the D2 period. (**e**,**j**,**l**) are contribution rates of driving factors of principal components in the IIA2, IIA3, and IIA4 regions in the D2 period. The red font indicates the highest R^2 values, the white font represents a significant coefficient below the 0.05 level, and the red bars indicate no contribution.

Table 5. Results of the factor detection in Fujian from D1 to D2.

Factor Type	Factors	IIA2		IIA3		IIA4	
		D1	D2	D1	D2	D1	D2
Human Activities	VPD	0.318	0.424	0.106	0.337	0.073	0.138
	RD	0.190	0.184	0.061	0.017 **	0.032 *	0.046
	POP	0.293	0.182	0.100	0.211	0.171	0.118
	GDP	0.244	0.246	0.117	0.144	0.239	0.162
Rainfall	R95p	0.342	0.222	0.197	0.304	0.232	0.285
	R99p	0.483	0.396	0.181	0.304	0.190	0.193
	Rx1day	0.041 **	0.394	0.152	0.344	0.238	0.281
	P50	0.213	0.190	0.208	0.261	0.179	0.285
Surface Environment	VFC	0.113	0.096	0.070	0.038	0.020 **	0.006 **
	LU	0.085	0.032 **	0.016 **	0.016 *	0.020 **	0.013 **
	ST	0.084	0.049 **	0.026 **	0.009 **	0.036 *	0.017 **
	ELE	0.078	0.036 **	0.049	0.024	0.079	0.023 **
	FL	0.050 **	0.061 **	0.041 **	0.067	0.091	0.080

Note: ** and * indicate significant coefficients exceeding the 0.05 and 0.01 levels, respectively.

3.3. Sensitivity Analysis

The sensitivity of the flash flood points to human activities (GDP and VPD) and precipitation (R95P and Rx1day) was analyzed by GTWR, and these four driving factors had a greater driving force for Fujian flash floods in the D1 and D2 periods than other nine driving factors. These results show that the mean R^2 adjusted value was 0.695, the value of the bandwidth was 0.115, and the Akaike information criterion (AIC) value was less than −3000, which reflected the preferable fitting degree of the GTWR model. From the perspective of the GDP (Figure 7a,e), the sensitive regions increased from D1 to D2. There was low sensitivity and moderate sensitivity in the Ningde areas, and the bordering areas of Sanming and Nanping increased significantly. For the VPD (Figure 7b,f), the moderate sensitivity and the high sensitivity in the bordering areas of Sanming and Nanping increasing significantly. In contrast, the sensitive areas in the southwest of Ningde were markedly reduced. From the perspective of R95p (Figure 7c,g), there was moderate sensitivity and high sensitivity in Ningde areas, and the bordering areas of Sanming and Nanping increased significantly. For the Rx1day (Figure 7d,h), except for the coast of Fujian Province (Quanzhou, Putian Fuzhou, and Ningde), the overall sensitivity of Fujian Province was weakened. From an overall perspective, flash floods were highly sensitive to the GDP, VPD, R95p, and Rx1day in Quanzhou.

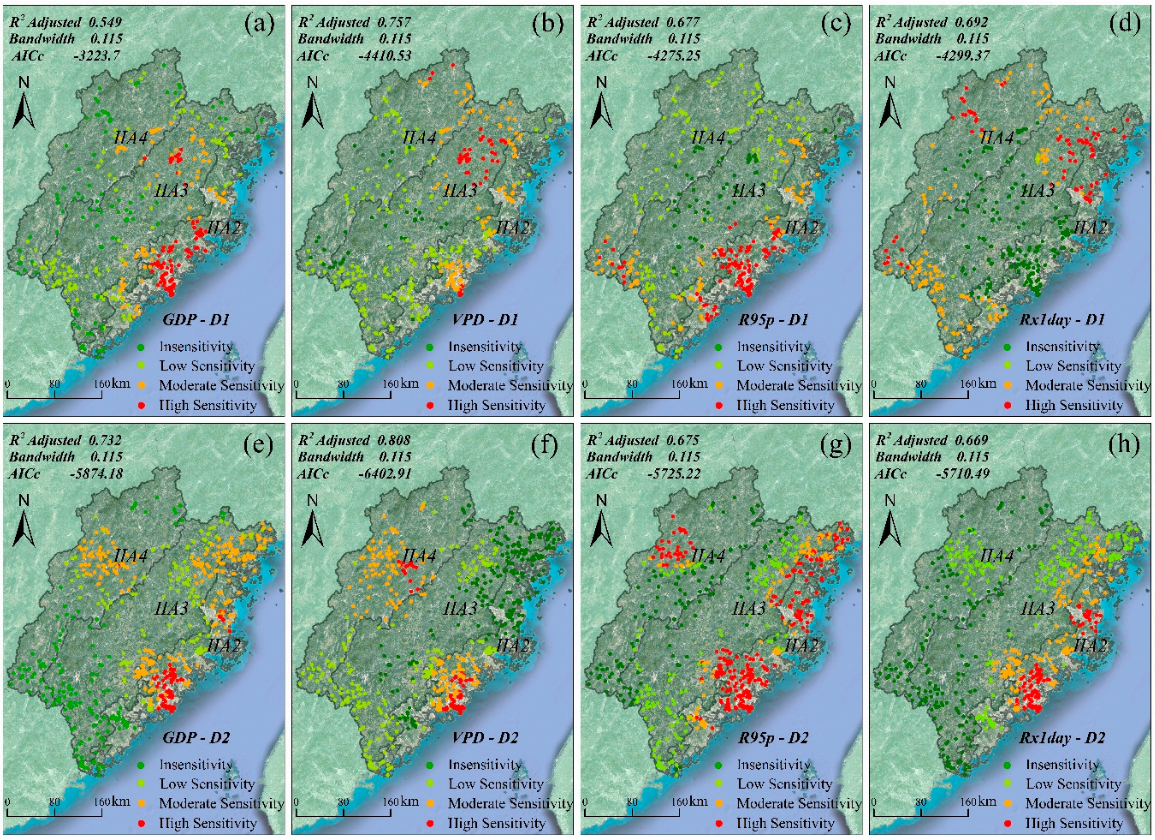

Figure 7. The sensitivity of flash flood to the (**a**) GDP, (**b**) POP, (**c**) R95p, and (**d**) Rx1day in the D1 period and the sensitivity of flash floods to the (**e**) GDP, (**f**) VPD, (**g**) R95p, and (**h**) Rx1day in the D2 period using GTWR.

4. Discussion

4.1. Spatiotemporal Patterns of Flash Floods

In this study, we revealed the significant yearly, monthly, and interannual variations of flash floods in Fujian Province. The flash floods showed an increasing tendency from 1951 to 2015 (Figure 2a). In particular, after 1980, the quantity of flash floods increased sharply (Figure 2b). The pattern is consistent with that of Sichuan Province in China [28,29]. Possible reasons include intensified human activity and increased extreme precipitation events in Fujian [63]. Undeniably, another possibility is that the quantity of flash floods was inaccurate due to unrecorded flash flood disasters prior to 1980. In addition, the months of flash floods in different GRs were not consistent (Figure 2d–f), and in some months, high frequency flash floods were often accompanied by heavy rainfall. That is, precipitation contributed significantly to flash floods [64]. Previous studies reported that flash floods mainly occurred in July and August in Tibet [26], and that they were concentrated in June, July, August, and September in Sichuan [28]. These differences are likely due to the precipitation being a huge driving force for the occurrence of flash floods [65], and different unique climatic conditions and geographical environments in those regions cause significant differences in the spatiotemporal distribution of precipitation [66,67].

The SDE analysis result signified that the overall spatial variation trend of flash floods was broadened from the coastal regions to the inland regions from the 1950s to the 2010s (Figure 3). Previous studies revealed an obvious increasing trend of extreme precipitation in northern, central, and southeastern coastal regions of Fujian [68]. Moreover, intensified human activity and increased precipitation after the 1980s led to changes in the precipitation pattern and surface runoff processes [69,70], indirectly causing the occurrence of flash floods. It is also possible that flash floods were not recorded because human footprints were rare in the IIA3 or IIA4 regions before the 1980s.

This was especially true in region IIA2, with high human activities, and flash floods were mainly concentrated in the central and eastern regions of Fuzhou and Quanzhou, the northeastern regions of Xiamen, the entire territory of Zhangzhou and Ningde, the southern regions of Longyan, and the northern regions of Sanming (Figure 3). Additionally, from Figures 4 and 5, we found that high intensity precipitation, dense population, and a developed economy were characteristics of these regions. Thus, it could be seen that the occurrence of flash floods was primarily affected by precipitation and human activity.

4.2. Driving Factors Influencing Flash Floods

4.2.1. Coastal Low Mountains, Hills, and Plain Regions of Fujian (IIA2)

The northern area of IIA2 was obviously affected by extreme precipitation events from D1 to D2 (Figure 4). The mean Q values of the precipitation indicator were 0.346 and 0.301, respectively. These results were attributed to the strongest influence on the extreme precipitation by the El Niño-southern oscillation, and the non-stationary characteristic of the extreme precipitation in this region [68,71]. In addition, this region is densely populated, with a developed economy (Figure 5), and the mean Q value of the human activity indicators was 0.26, which was the highest mean Q value of the three geomorphic regionalization values. The reason for this was that numerous external populations have been attracted to the coastal regions in Fujian Province since the reform and opening-up [72]. Subsequently, with deforestation, urban expansion, and wasteland reclamation, the natural cover protection for the land was removed [73], surface runoff processes were changed and rainwater confluence times were shortened [64], and flash floods were prone to occur under the influence of precipitation. These are the reasons why the human activity indicator and the precipitation indicator had a great driving force on flash floods in the interaction detection analysis (Figure 6). Specifically, the Q values of VPD and Rx1day increased significantly from D1 to D2 (Table 5), and the contribution rate exceeded 10% of the driving factors from the precipitation and human activity indicators for both D1 and D2 periods (Figure 6), These results indicated that the interaction of precipitation and human activity was responsible for the occurrence of flash floods in the IIA2 region.

4.2.2. Low-Middle Mountains, Hills, and Valley Region in Central Fujian (IIA3)

This region was characterized by an obvious spatial distribution of precipitation due to the obstruction of the atmospheric circulation by several mountain ranges [74,75]. Furthermore, the precipitation indicator had the highest mean Q value in both periods, with an obvious increase from 0.185 to 0.303 (Table 5). A possible reason for this is that the IIA3 region had a lower population activity relative to the IIA2 region (Figure 5), with intensification of the global atmospheric water cycle [76], and several mountain ranges affecting the movement of the southeastern monsoon, giving rise to orographic rain [66], and resulting in more frequent precipitation events [77]. In addition, a series of policies were used to promote the coordinated development of the inland and coastal regions in Fujian Province, such as industry regional transference and cross-regional resource flows [78]. It is worth emphasizing that the Q value of the VPD increased significantly from 0.106 to 0.337, and the Q value of P50 increased significantly from 0.152 to 0.344. The obvious changes were attributed to the development of urban construction. The natural cover protection was damaged [79], the urban impermeable area increased, and river gullies were occupied [80], with the result of reduced precipitation thresholds required for a flash flood to occur [29].

4.2.3. Low-Middle Mountains, Hills and Valley Region in Wuyi Mountains (IIA4)

Unlike regions IIA2 and IIA3, IIA4 has a sparse population and underdeveloped economy (Figure 5). The reason for the abundant precipitation in this area is that the atmospheric circulation is blocked by the Wuyi Mountains [81]. Through the driving factor detection (Table 5) and multiple factor detection (Figure 6), we found that human activities had a low effect on flash floods. These possible reasons were likely due to the fact that the spatial distributions of the POP and GDP remained almost unchanged in both periods, the human activity intensity was the weakest in three geomorphic regionalization (Figures 5 and 6), and the original eco-environment structure was relatively complete [82]. As illustrated in Figure 4, from D1 to D2, we found that the intensity of the extreme precipitation increased in this region, and the contribution rates were dominated by precipitation indicators (Figure 6). These results indicated that precipitation was responsible for the occurrence of flash floods in this region.

From the perspective of the whole territory of Fujian Province, the driving forces of human activity indicators for flash floods gradually weakened from IIA2 to IIA3 and to IIA4; these differences were mainly related to the intensity of human activity. In contrast, the contribution of the precipitation indicators gradually strengthened from IIA2 to IIA3 and to IIA4. These transitions were caused by the significant spatial distribution differences of precipitation, and this spatial distribution was closely related to the topography. In particular, the effects of the monsoon season (March to June) and the typhoon season (July to September) are inconsistent in different regions [32]. Additionally, the extreme precipitation caused by tropical cyclones was strongly affected by the topography [83]. These were the reasons for the significant differences in the times and quantities of flash floods in different GRs. However, the influence of surface environmental factors on flash floods was very small in both periods. These results indicated that the surface environment was only a carrier for the occurrence of flash floods, not the decisive factor [84]. From the interaction detection (Figure 6), we found that the closer the distance to the densely populated coastal areas, the more the driving factors of flash floods result from human activity. When humans transform nature, they also destroy the natural self-regulation ability and increase the exposure of humans to natural disasters [85].

4.3. Sensitivity Analysis of the Flash Floods

The sensitivity analysis of flash floods to GDP, VPD, R95p, and Rx1day was used to reflect the response of flash floods to human activity and precipitation in Fujian Province. Based on Figure 7, we found that flash floods in Quanzhou had moderate and high sensitivity to the four driving factors in the two periods. After the reform and opening-up, Quanzhou Port played an important role in China's foreign trade [86]. However, with the economic development and infrastructure construction, the frequency of flash floods gradually increased. The good geographical conditions and advantages made Quanzhou rapidly grow into a port city with strong economic power [87]. This is why the flash floods were more sensitive to VPD than to GDP in the D1 period. In the 21st century, measures such as "industry regional transfer" were used to release the development pressure of coastal regions and promote economic development in inland areas [78]. Although the economy of the inland areas developed, it also destroyed the eco-environment and led to frequent flash floods. Additionally, the bordering areas of Sanming and Nanping have rich mineral resources, which played an important role in the local economic development, while the local ecological environment was also destroyed [88]. Flash floods were prone to occur under the influence of heavy precipitation. In particular, regarding the northeastern regions of Fujian in the D2 period, the precipitation had a more significant effect than that in the D1 period. Furthermore, with the implementation of some policies to promote the regional coordinated development in Fujian Province, these regions developed rapidly after entering the 21st century [89]. This is the reason for the moderate and high sensitivity of flash floods to R95p, Rx1day, and GDP in these regions. Therefore, it follows that the hazard factors of flash floods in Fujian Province in different periods and different regions had significant differences.

4.4. Limitations of the Current Study

In this study, we conducted a preliminary analysis of the spatiotemporal distribution and driving factors of the flash floods in Fujian Province, and we detected the sensitivity of flash floods to VPD, GDP, R95p, and Rx1day. Nevertheless, there are some deficiencies in the current study. First, there was a lack of comprehensive record data before 1980, which is why the driving factor analysis began in 1981. Second, Fujian Province is one of the areas seriously affected by tropical cyclones, but the driving effect of tropical cyclones on extreme precipitation and flash floods was not researched in this study. Moreover, we adopted daily precipitation data instead of sub-daily precipitation data, which did not accurately reflect the effects of short-term precipitation on flash floods. Finally, the analysis of the driving factors of flash floods based on three-grade GR was not very accurate because of the spatial heterogeneity of the flash flood driving factors. Despite these deficiencies, this work has provided primary references for the spatiotemporal pattern of flash floods in Fujian Province and has improved the public awareness of flash floods.

5. Conclusions

Flash floods are serious, catastrophic natural disasters that can occur practically anywhere. Areas susceptible to flash floods have been identified as a crucial consideration worldwide. The spatiotemporal exploration and driving force analysis of flash flood are effective means of predicting and controlling these events. In this study, a long-term series of flash flood events was used to analyze the spatiotemporal variation in Fujian Province from 1951 to 2015. Three-grade GR was used to detect the single factor explanatory power and the contribution rate of multiple driving factors that interacted with the spatial patterns of flash floods from D1 to D2. Moreover, the sensitivities of flash floods to GDP, VPD, R95p, and P50 were explored. Three main conclusions were summarized as follows.

(1) The quantity of flash floods has risen sharply since the 1980s, and the frequency of flash floods from IIA2 to IIA4 has decreased gradually. Moreover, similar to precipitation, the months of flash floods in different GRs were not consistent. The main reason for this is that the spatiotemporal distribution of precipitation in Fujian Province is obviously affected by the topography, and human activities promoted the occurrence of flash floods, particularly in the IIA2 region.

(2) In the IIA2 region, the high-incidence area of flash floods was mainly attributed to the interaction of human activity and precipitation, causing frequent flash floods. In the IIA3 region, precipitation was mainly responsible for the occurrence of flash floods, and the impact of human activities could not be ignored after entering the 21st century. Regarding the IIA4 region, due to the weak intensity of human activities in the region and the obstruction of atmospheric circulation by the Wuyi Mountain, precipitation has become a major factor in the occurrence of flash floods.

(3) The sensitivity analysis results revealed that the hazard factors of flash floods in different periods and different regions had significant differences in Fujian Province. These differences were mainly attributed to the different intensities of human activity and regional climates in different regions.

Based on the research, the forecast of extreme precipitation and the prevention and control of flash floods should be strengthened, especially in coastal areas. Additionally, the economic development model of coastal areas should be improved, the ecological environment of inland areas should be protected, and the harmonious development of man and nature should be promoted. In addition, the result indicated that for some regions, regional climate and human activity were the most important factors influencing the timing and location of flash floods in Fujian Province. Overall, this study provides a reference to assist governments, planners, and engineers to perform the proper actions in Fujian Province and to prevent and mitigate flash floods in the future.

Author Contributions: Conceptualization, Junnan Xiong and Quan Pang; Data curation, Junnan Xiong and Weiming Cheng; Formal analysis, Quan Pang; Funding acquisition, Junnan Xiong, Chunkun Fan and Weiming Cheng; Resources, Junnan Xiong and Weiming Cheng; Supervision, Weiming Cheng and Yuanrong He; Writing—original draft, Junnan Xiong and Quan Pang; Writing—review & editing, Quan Pang, Chongchong Ye, Yunliang Zhao and Yifan Cao. All authors have read and agreed to the published version of the manuscript.

Funding: This research was funded by the Strategic Priority Research Program of the Chinese Academy of Sciences, Grant No. XDA20030302, the Science and Technology Project of Xizang Autonomous Region, Grant No. XZ201901-GA-07, Open Subject of Big Data Institute of Digital Natural Disaster Monitoring in Fujian, Grant No. NDMBD2018003, China Institute of water Resources and Hydropower Research, Grant No. SHZH-IWHR-57, and Southwest Petroleum University of Science and Technology Innovation Team Projects, Grant No. 2017CXTD09.

Conflicts of Interest: The authors declare no conflict of interest.

References

1. Tang, C.; Zhu, J. A GIS Based Regional Torrent Risk Zonation. *Acta Geogr. Sin.* **2005**, *60*, 87–94.
2. Guo, L.; Zhang, X.L. Achievements and Preliminary Analysis on China National Flash Flood Disasters Investigation and Evaluatio. *J. Geo-Inf. Sci.* **2017**, *19*, 1548–1556.
3. Ashley, S.T.; Ashley, W.S. Flood Fatalities in the United States. *J. Appl Meteorol. Climatol.* **2008**, *47*, 805–818. [CrossRef]
4. Špitalar, M.; Gourley, J.J.; Lutoff, C.; Kirstetter, P.-E.; Brilly, M.; Carr, N. Analysis of flash flood parameters and human impacts in the US from 2006 to 2012. *J. Hydrol.* **2014**, *519*, 863–870. [CrossRef]
5. Li, C.-J.; Chai, Y.-Q.; Yang, Y.-S.; Li, H.-R. Spatio-temporal distribution of flood disasters and analysis of influencing factors in Africa. *Nat. Hazards* **2016**, *82*, 721–731. [CrossRef]
6. Martín-Vide, J.P.; Llasat, M.C. The 1962 flash flood in the Rubí stream (Barcelona, Spain). *J. Hydrol.* **2018**, *566*, 441–454. [CrossRef]
7. Liu, Y.; Yang, Y. Spatial Distribution of Major Natural Disasters of China in Historical Period. *Acta Geogr. Sin.* **2012**, *67*, 291–300.
8. Xu, S.; Wang, J.; Shi, C.; Yan, J. Research of the Natural Disaster Risk on Coastal Cities. *Acta Geogr. Sin.* **2006**, *61*, 127–138.
9. Guo, L.; Ding, L.; Sun, D. Key technologies and applications of flash flood disaster investigation and assessment in China. *China Flood Drought Manag.* **2018**, *28*, 7–11, 32.
10. Nikolopoulos, E.I.; Destro, E.; Bhuiyan, M.A.E.; Borga, M.; Anagnostou, E.N. Evaluation of predictive models for post-fire debris flow occurrence in the western United States. *Nat. Hazards Earth Syst. Sci.* **2018**, *18*, 2331–2343. [CrossRef]
11. Guo, L.; Liu, J.C.; Ding, L.Q. Working plan for mountain flood investigation and evaluation in China. *China Water Resour.* **2012**, *23*, 10–12.
12. Zhang, Y.; Cheng, W.; Wang, N. Risk assessment of mountain flood based on GIS and Logistic regression model. *China Flood Drought Manag.* **2018**, *28*, 21–26, 30.
13. Costache, R.; Pham, Q.B.; Sharifi, E.; Linh, N.T.T.; Abba, S.I.; Vojtek, M. Flash-Flood Susceptibility Assessment Using Multi-Criteria Decision Making and Machine Learning Supported by Remote Sensing and GIS Techniques. *Remote Sens.* **2019**, *12*, 106. [CrossRef]
14. Shehata, M.; Mizunaga, H. Flash Flood Risk Assessment for Kyushu Island, Japan. *Environ. Earth Sci.* **2018**, *77*, 76. [CrossRef]
15. Shehata, M.; Mizunaga, H. Geospatial analysis of surface hydrological parameters for Kyushu Island, Japan. *Nat. Hazards* **2019**, *9*, 33–52. [CrossRef]
16. Xiong, J.; Li, J.; Cheng, W.; Wang, N.; Guo, L. A GIS-Based Support Vector Machine Model for Flash Flood Vulnerability Assessment and Mapping in China. *ISPRS Int. J. Geo-Inf.* **2019**, *8*, 297. [CrossRef]
17. Varlas, G.; Anagnostou, M.N.; Spyrou, C.; Papadopoulos, A.; Kalogiros, J.; Mentzafou, A.; Michaelides, S.; Baltas, E.; Karymbalis, E.; Katsafados, P. A Multi-Platform Hydrometeorological Analysis of the Flash Flood Event of 15 November 2017 in Attica, Greece. *Remote Sens.* **2018**, *11*, 45. [CrossRef]
18. Hoedjes, J.; Kooiman, A.; Maathuis, B.; Said, M.; Becht, R.; Limo, A.; Mumo, M.; Nduhiu-Mathenge, J.; Shaka, A.; Su, B. A Conceptual Flash Flood Early Warning System for Africa, Based on Terrestrial Microwave Links and Flash Flood Guidance. *ISPRS Int. J. Geo-Inf.* **2014**, *3*, 584–598. [CrossRef]
19. Hoang, T.V.; Chou, T.Y.; Nguyen, N.T.; Fang, Y.M.; Yeh, M.L.; Nguyen, Q.H.; Nguyen, X.L. A Robust Early Warning System for Preventing Flash Floods in Mountainous Area in Vietnam. *ISPRS Int. J. Geo-Inf.* **2019**, *8*, 228. [CrossRef]
20. Tyrna, B.; Assmann, A.; Fritsch, K.; Johann, G. Large-scale high-resolution pluvial flood hazard mapping using the raster-based hydrodynamic two-dimensional model FloodAreaHPC. *J. Flood Risk Manag.* **2018**, *11*, S1024–S1037. [CrossRef]
21. Henriksen, H.J.; Roberts, M.J.; van der Keur, P.; Harjanne, A.; Egilson, D.; Alfonso, L. Participatory early warning and monitoring systems: A Nordic framework for web-based flood risk management. *Int. J. Disaster Risk Reduct.* **2018**, *31*, 1295–1306. [CrossRef]
22. Gan, B.R.; Liu, X.N.; Yang, X.G. The impact of human activities on the occurrence of mountain flood hazards: Lessons from the 17 August 2015 flash flood/debris flow event in Xuyong County, south-western China. *Geomat. Nat. Hazards Risk* **2018**, *9*, 816–840. [CrossRef]

23. Wang, Y.; Cui, P.; Wang, Z.; Liang, S. Study on the formation and characteristics of height of debris flow head. *J. Hydraul. Eng.* **2017**, *48*, 437–479.
24. Papagiannaki, K.; Lagouvardos, K.; Kotroni, V.; Bezes, A. Flash flood occurrence and relation to the rainfall hazard in a highly urbanized area. *Nat. Hazards Earth Syst. Sci.* **2015**, *15*, 1859–1871. [CrossRef]
25. Xiong, J.; Ye, C.; Cheng, W.; Guo, L.; Zhou, C.; Zhang, X. The Spatiotemporal Distribution of Flash Floods and Analysis of Partition Driving Forces in Yunnan Province. *Sustainability* **2019**, *11*, 2926. [CrossRef]
26. Xiong, J.; Gong, Y.; Cheng, W. Temporal and Spatial Distribution Characteristics of Mountain Floods in Tibet, China in Recent 30 Years. *Mt. Res.* **2018**, *36*, 557–570.
27. Djimesah, I.E.; Okine, A.N.D.; Kissi Mireku, K. Influential factors in creating warning systems towards flood disaster management in Ghana: An analysis of 2007 Northern flood. *Int. J. Disaster Risk Reduct.* **2018**, *28*, 318–326. [CrossRef]
28. Xiong, J.; Zhao, Y.; Cheng, W. Temporal-spatial Distribution and the Influencing Factors of Mountain-Flood Disasters in Sichuan Province. *Geo-Inf. Sci.* **2018**, *20*, 1443–1456.
29. Liu, Y.; Yuan, X.; Guo, L.; Huang, Y.; Zhang, X. Driving Force Analysis of the Temporal and Spatial Distribution of Flash Floods in Sichuan Province. *Sustainability* **2017**, *9*, 1527. [CrossRef]
30. Wang, B.; Wang, Y. The development of economic gravity center and spatial difference of economy in Fujian from 1989 to 2008. *Geogr. Res.* **2011**, *30*, 1882–1890.
31. Zhong, S.; Wang, C.; Yu, Z.; Yang, Y.; Huang, Q. Spatiotemporal Exploration and Hazard Mapping of Tropical Cyclones along the Coastline of China. *Adv. Meteorol.* **2018**, *2018*, 1–15. [CrossRef]
32. Zhang, S.; Chang, T.; Wang, Y. Spatial and Seasonal Precipitation Variability in Eastern Fujian Based on Automatic Station Observation Data. *Sens. Mater.* **2018**, *30*, 525–538. [CrossRef]
33. China Statistical Yearbook 2018. Available online: http://www.stats.gov.cn/tjsj/ndsj/2018/indexch.htm (accessed on 30 December 2019).
34. Zhao, Z. The Relation between Basic Geomorphic Characters and Agricultural Production in Fujian. *Acate Geogr. Sin.* **1993**, *48*, 143–151.
35. Zhao, Z.B. Features of Fujian's Mountain Environment and Problems of Its Development. *Acta Geogr. Sin.* **1984**, *39*, 409–417.
36. Zhou, Y.; Xiao, F.; Luo, Y.; Zhao, S. Study on Tropical Cyclone Potential Impact Index in China. *Acta Geogr. Sin.* **2011**, *66*, 367–375.
37. Dong, G.; Wei, J.; Hu, G. Practice of mountain flood prevention in Fujian Province. *China Water Resour.* **2012**, *13*, 47–48.
38. The National Meteorological Information of China (CMA). Available online: http://data.cma.cn/data/detail/dataCode/A.0029.0001.html (accessed on 30 December 2019).
39. The Expert Team on Climate Change Detection and Indices (ETCCDI). Available online: http://cccma.seos.uvic.ca/ETCCDI/list27indices.html (accessed on 30 December 2019).
40. The Geospatial Data Cloud Site, Computer Network Information Center, Chinese Academy of Sciences (GDC). Available online: http://www.gscloud.cn (accessed on 30 December 2019).
41. The Data Center for Resources and Environmental Sciences, Chinese Academy of Sciences (RESDC). Available online: http://www.resdc.cn (accessed on 30 December 2019).
42. Kendall, M.G.; Stuart, A. The Advanced Theory of Statistics: Design and Analysis, and time-series. *J. R. Stat. Soc. Ser. A* **1984**, *147*, 523.
43. Gocic, M.; Trajkovic, S. Analysis of changes in meteorological variables using Mann-Kendall and Sen's slope estimator statistical tests in Serbia. *Glob. Planet. Chang.* **2013**, *100*, 172–182. [CrossRef]
44. Peng, Y.; Song, J.; Cui, T.; Cheng, X. Temporal–spatial variability of atmospheric and hydrological natural disasters during recent 500 years in Inner Mongolia, China. *Nat. Hazards* **2017**, *89*, 441–456. [CrossRef]
45. Lefever, D.W. Measuring Geographic Concentration by Means of the Standard Deviational Ellipse. *Am. J. Sociol.* **1926**, *32*, 88–94. [CrossRef]
46. Shi, Y.; Matsunaga, T.; Yamaguchi, Y.; Li, Z.; Gu, X.; Chen, X. Long-term trends and spatial patterns of satellite-retrieved PM2.5 concentrations in South and Southeast Asia from 1999 to 2014. *Sci Total Environ.* **2018**, *615*, 177–186. [CrossRef] [PubMed]
47. Shrestha, A.B.; Bajracharya, S.R.; Sharma, A.R.; Duo, C.; Kulkarni, A. Observed trends and changes in daily temperature and precipitation extremes over the Koshi river basin 1975–2010. *Int. J. Climatol.* **2017**, *37*, 1066–1083. [CrossRef]

48. Jiang, J.; Mo, D.; Lu, J.; Liao, Y.; Lu, P.; Ren, X. Holocene geomorphic evolution of Taiyuan Basin in Shanxi Province and its influence on ancient human settlement distribution. *J. Palaeogr.* **2016**, *18*, 895.
49. Lu, H. Progress in geomorphology and future study: A brief review. *Prog. Geogr.* **2018**, *37*, 8–15.
50. Shafapour Tehrany, M.; Pradhan, B.; Jebur, M.N. Spatial prediction of flood susceptible areas using rule based decision tree (DT) and a novel ensemble bivariate and multivariate statistical models in GIS. *J. Hydrol.* **2013**, *504*, 69–79. [CrossRef]
51. Wang, Z.; Lai, C.; Chen, X.; Yang, B.; Zhao, S.W.; Bai, X.Y. Flood Hazard Risk Assessment Model Based on Random Forest. *J. Hydrol.* **2015**, *527*, 1130–1140. [CrossRef]
52. Cosby, B.J.; Hornberger, G.M.; Clapp, R.B.; Ginn, T.R. A statistical exploration of the relationships of soil moisture characteristics to the physical properties of soils. *Water Resour. Res.* **1984**, *20*, 682–690. [CrossRef]
53. Cheng, W.; Zhou, C.; Li, B.; Shen, Y. Geomorphological Regionalization Theory System and Division Methodology of China. *Acta Geogr. Sin.* **2019**, *74*, 839.
54. Wang, J.F.; Xu, C.D. Geodetector: Principle and prospective. *Acate Geogr. Sin.* **2017**, *72*, 116–134.
55. Wang, J.F.; Li, X.H.; Christakos, G.; Liao, Y.L.; Zhang, T.; Gu, X.; Zheng, X.Y. Geographical Detectors-Based Health Risk Assessment and its Application in the Neural Tube Defects Study of the Heshun Region, China. *Int. J. Geogr. Inf. Sci.* **2010**, *24*, 107–127. [CrossRef]
56. Qiao, P.; Yang, S.; Lei, M.; Chen, T.; Dong, N. Quantitative analysis of the factors influencing spatial distribution of soil heavy metals based on geographical detector. *Sci. Total Environ.* **2019**, *664*, 392–413. [CrossRef] [PubMed]
57. Abdi, H.; Williams, L.J. Principal component analysis. *Wiley Interdiscip. Rev. Comput. Stat.* **2010**, *2*, 433–459. [CrossRef]
58. Uyanık, G.K.; Güler, N. A Study on Multiple Linear Regression Analysis. *Procedia Soc. Behav. Sci.* **2013**, *106*, 234–240. [CrossRef]
59. Huang, B.; Wu, B.; Barry, M. Geographically and temporally weighted regression for modeling spatio-temporal variation in house prices. *Int. J. Geogr. Inf. Sci.* **2010**, *24*, 383–401. [CrossRef]
60. Xu, C.D.; Xiao, G.X.; Li, J.M.; Cao, H.X. Spatiotemporal patterns and risk factors concerning hepatitis B virus infections in the Beijing-Tianjin-Hebei area of China. *Epidemiol. Infect.* **2019**, *147*, 1–8. [CrossRef]
61. Du, Z.; Wu, S.; Zhang, F.; Liu, R.; Zhou, Y. Extending geographically and temporally weighted regression to account for both spatiotemporal heterogeneity and seasonal variations in coastal seas. *Ecol. Inform.* **2018**, *43*, 185–199. [CrossRef]
62. Zhang, X.; Huang, B.; Zhu, S. Spatiotemporal Influence of Urban Environment on Taxi Ridership Using Geographically and Temporally Weighted Regression. *ISPRS Int. J. Geo-Inf.* **2019**, *8*, 23. [CrossRef]
63. Stott, P.A.; Gillett, N.P.; Hegerl, G.C.; Karoly, D.J.; Stone, D.A.; Zhang, X.; Zwiers, F. Detection and attribution of climate change: A regional perspective. *Wiley Interdiscip. Rev. Clim. Chang.* **2010**, *1*, 192–211. [CrossRef]
64. Cortès, M.; Turco, M.; Llasat-Botija, M.; Llasat, M.C. The relationship between precipitation and insurance data for floods in a Mediterranean region (northeast Spain). *Nat. Hazards Earth Syst. Sci.* **2018**, *18*, 857–868. [CrossRef]
65. Hou, J.; Guo, K.; Liu, F.; Han, H.; Liang, Q.; Tong, Y.; Li, P. Assessing Slope Forest Effect on Flood Process Caused by a Short-Duration Storm in a Small Catchment. *Water* **2018**, *10*, 1256. [CrossRef]
66. Zhang, H.; Sun, J.; Xiong, J. Spatial-Temporal Patterns and Controls of Evapotranspiration across the Tibetan Plateau (2000–2012). *Adv. Meteorol.* **2017**, *2017*, 1–12. [CrossRef]
67. Xiong, J.; Yong, Z.; Wang, Z.; Cheng, W.; Li, Y.; Zhang, H.; Ye, C.; Yang, Y. Spatial and Temporal Patterns of the Extreme Precipitation across the Tibetan Plateau (1986–2015). *Water* **2019**, *11*, 1453. [CrossRef]
68. Gao, L.; Huang, J.; Chen, X.; Chen, Y.; Liu, M. Risk of Extreme Precipitation under Nonstationarity Conditions during the Second Flood Season in the Southeastern Coastal Region of China. *J. Hydrometeorol.* **2017**, *18*, 669–681. [CrossRef]
69. Yin, J.; Gentine, P.; Zhou, S.; Sullivan, S.C.; Wang, R.; Zhang, Y.; Guo, S. Large increase in global storm runoff extremes driven by climate and anthropogenic changes. *Nat. Commun.* **2018**, *9*, 4389–4398. [CrossRef] [PubMed]
70. Roa-García, M.C.; Brown, S.; Schreier, H.; Lavkulich, L.M. The role of land use and soils in regulating water flow in small headwater catchments of the Andes. *Water Resour. Res.* **2011**, *47*, 5–16. [CrossRef]
71. Chen, S.; Zha, X. Effects of the ENSO on rainfall erosivity in the Fujian Province of southeast China. *Sci. Total Environ.* **2018**, *621*, 1378–1388. [CrossRef] [PubMed]

72. Xiao, Z.H. Forty Years of Reform and Opening-up and the Great Flow of Population in China. *Popul. Soc.* **2019**, *35*, 30–38.
73. Lean, J.; Warrilow, D.A. Simulation of The Regionl Climatic Impact of Amazon Deforestation. *Nature* **1989**, *342*, 411–413. [CrossRef]
74. Huang, Y.; Duan, Y.; Yu, H. A Study of the Impact of Terrain on the Precipitation of "KROSA". *Meteorol. Mon.* **2009**, *35*, 3–10.
75. Pang, M.; Si, G. Influence of The Regional Scale Topography on The Climatalogical Distribution of Precipitation. *J. Trop. Meteorol.* **1993**, *9*, 370–374.
76. Xue, D.; Lu, J.; Ruby, L.L.; Zhang, Y. Response of the Hydrological Cycle in Asian Monsoon Systems to Global Warming Through the Lens of Water Vapor Wave Activity Analysis. *Geophys. Res. Lett.* **2018**, *45*, 904–912. [CrossRef]
77. King, A.D.; Donat, M.G.; Fischer, E.M.; Hawkins, E.; Alexander, L.V.; Karoly, D.J.; Dittus, A.J.; Lewis, S.C.; Perkins, S.E. The timing of anthropogenic emergence in simulated climate extremes. *Environ. Res. Lett.* **2015**, *10*, 1–9. [CrossRef]
78. Fu, Y. Industrial transfer trend in the eastern coastal areas: Based on the investigation of Zhejiang. *Economist* **2011**, *10*, 84–90.
79. Yun, Y.; Shi, P.; Liu, Y. Impact of Land Use Chang on Urban Flood. *J. Nat. Disasters* **2003**, *12*, 6–13.
80. Mao, H.; Yan, X.; Xiong, Z. An Overview of Impacts of Land Use Change on Climate. *Clim. Environ. Res.* **2011**, *16*, 513–524.
81. Shen, X.; Shou, S.; Xu, Z. Numerical Simulation and Analysis of Influence of Complex Topography on a Fujian Rainstorm. *J. Nanjing Inst. Meteorol.* **2008**, *31*, 546–5544.
82. Tang, W.; Zhou, T.; Sun, J.; Li, Y.; Li, W. Accelerated Urban Expansion in Lhasa City and the Implications for Sustainable Development in a Plateau City. *Sustainability* **2017**, *9*, 1499. [CrossRef]
83. Qiu, W.; Ren, F.; Wu, L.; Chen, L.; Ding, C. Characteristics of tropical cyclone extreme precipitation and its preliminary causes in Southeast China. *Meteorol. Atmos. Phys.* **2018**, *131*, 613–626. [CrossRef]
84. Liu, Y.; Yang, Z.; Huang, Y.; Liu, C. Spatiotemporal evolution and driving factors of China's flash flood disasters since 1949. *Sci. China Earth Sci.* **2018**, *61*, 1804–1817. [CrossRef]
85. Du, S.; Cheng, X.; Huang, Q.; Chen, R.; Ward, P.J.; Aerts, J.C.J.H. Brief communication: Rethinking the 1998 China floods to prepare for a nonstationary future. *Nat. Hazards Earth Syst. Sci.* **2019**, *19*, 715–719. [CrossRef]
86. Shi, T.; Xu, H.; Wang, S.; Fang, C.; Lin, Z.; Wang, M.; Tang, F. Remote Sensing Study of Coastline Dynamics of Quanzhou Port:Starting Point of the Ancient Maritime Silk Road. *J. Geo-Inf. Sci.* **2017**, *19*, 407–416.
87. Huang, X.; Huang, M. Relationship between sustainable urban development and economic growth based on emergy analysis: A case study of Quanzhou City. *Prog. Geogr.* **2015**, *34*, 38–47.
88. Bawa, K.S.; Dayanandan, S. Socioeconomic factors and tropical deforestation. *Nature* **1997**, *386*, 562–563. [CrossRef]
89. Yi, Q. A Study on Path of Transformation and Upgrade of Fujian's Outward Economy. *Asia-Pac. Econ. Rev.* **2012**, *2*, 120–128.

© 2020 by the authors. Licensee MDPI, Basel, Switzerland. This article is an open access article distributed under the terms and conditions of the Creative Commons Attribution (CC BY) license (http://creativecommons.org/licenses/by/4.0/).